Proceedings of the 2005 IEEE
Engineering in Medicine and Biology 27th Annual Conference
Shanghai, China, September 1-4, 2005

Leukocyte segmentation and classification in blood-smear images

Herbert Ramoser*, Vincent Laurain*, Horst Bischof† and Rupert Ecker‡
*Advanced Computer Vision GmbH — ACV, Donau-City-Strasse 1, 1220 Wien, Austria, Email: herbert.ramoser@acv.ac.at
†Inst. for Computer Graphics and Vision, University of Technology, Graz, Austria, Email: bischof@icg.tu-graz.ac.at
‡TissueGnostics GmbH, Vienna, Austria, Email: rupert.ecker@tissuegnostics.com

***Abstract*— The detection and classification of leukocytes in blood smear images is a routine task in medical diagnosis. In this paper we present a fully automated approach to leukocyte segmentation that is robust with respect to cell appearance and image quality. A set of features is used to describe cytoplasm and nucleus properties. Pairwise SVM classification is used to discriminate between different cell types. Evaluation on a set of 1166 images (13 classes) resulted in 95% correct segmentations and 75% to 99% correct classification (with reject option).**

I. Introduction

Blood cell counting and blood film examination are widespread diagnostic techniques. A blood smear is obtained by drawing blood from a vein and placing a drop on a glass slide. The blood film is stained with a Romanowsky stain (e. g., Wright's, Giemsa, or May-Grünwald) and imaged with a transmission light microscope.

Typical cell types which can be found in blood smear images are erythrocytes (red blood cells), platelets, and leukocytes (white blood cells). See Fig. 1 for a sample image. During blood film examination, the individual types of leukocytes are enumerated; this is referred to as the differential count. Normal peripheral blood contains following types of leukocytes (the numbers in brackets give the typical proportion of the cell type): segmented neutrophil (40–75%), lymphocyte (25–33%), monocyte (2–8%), eosinophil granulocyte (1–4%), band neutrophil (1–3%), plasma cell (0.2–2.8%), basophil granulocyte (0.5%), and atypical lymphocyte. Other cell types which are observed in certain diseases include: metamyelocyte, myelocyte, promyelocyte, myeloblast, and erythroblast.

There is a vast amount of literature dedicated to differential blood counts. An automated system where cells are segmented using active contour models (snakes and balloons, initialized using morphological operators) is presented in [7]. Shape and texture features are used for classification. A two-step segmentation process is used in [12]. First the HSV-transformed image is clustered using k-means followed by an EM-algorithm. Shape, color, and texture are used for neural network classification. A mean-shift-based color segmentation procedure applied to leukocyte images is described in [1]. Segmentation is performed in the L*u*v* color space. A watershed-based segmentation is used in [3]. First a sub-image containing a leukocyte is separated from the cell image. The nucleus region is detected by scale-space filtering and the cytoplasm region by watershed clustering of the 3-D HSV histogram. A leukocyte segmentation based on thresholding is described in [4]. First thresholding provides initial labels to pixels in the blood cell images. Then the labels are adjusted with a shape detection method based on large regional context information to improve the segmentation. A classification approach using eigenimages is presented in [10]. The cells are adjusted for size and rotation. The eigencells are selected to minimize similarities among sets and classified using intensity-color information.

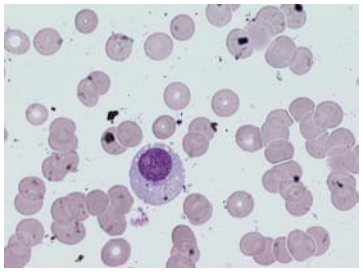

Fig. 1. Sample blood smear image. The leukocyte is the large cell in the image center (the cytoplasm is light blue and the nucleus is dark blue). The small circular cells are erythrocytes.

The results of these published methods show that the most crucial steps are proper cell segmentation and selection of discriminative features while the choice of classification method seems to have little influence on the obtainable classification accuracy. The problem of variable image quality is not addressed in any of these publications. We propose an adaptive leukocyte segmentation method followed by support vector machine classification using features describing nucleus shape and cell color statistics.

The remainder of the paper is structured as follows: in section II we describe a robust probability-based cell segmentation method, extracted cell features, and an SVM classification approach. Segmentation and classification results are given in section III. A discussion of the results and concluding remarks can be found in sections IV and V.

II. Methods

The approach of leukocyte classification consists of two parts: (1) the segmentation of leukocyte, cytoplasm, and nucleus; (2) the classification of the segmented leukocytes using a set of features. For the segmentation procedure we assume that the input image contains at least one leukocyte. The presence of a leukocyte in an image can, for example, be determined by analyzing the saturation component of pixels

0-7803-8740-6/05/$20.00 ©2005 IEEE.

in an image (the nucleus of a leukocyte has a high saturation compared to other cells).

A. Leukocyte segmentation

The segmentation of the blood smear images is split into several stages:

- detection of image background, potential nucleus regions, and other regions (e.g., erythrocyte and cytoplasm)
- suppression of image background color
- segmentation of individual leukocytes
- segmentation of every leukocyte into nucleus and cytoplasm

1) Nucleus-background separation: In practice the appearance of blood cells and image background varies strongly with respect to color and intensity. This behavior is, for example, caused by camera settings, varying illumination and aging stain. In order to make the cell segmentation robust with respect to these variations an adaptive procedure is used: the RGB input image is converted into the HSL color space. A k-means clustering procedure ($k = 3$) is used to assign every pixel to one of three clusters. These clusters correspond to nucleus (high saturation), background (high luminance, low saturation), and other cells (e. g., erythrocytes and leukocyte cytoplasm). Every pixel is assigned to one of these three classes using the properties of the cluster center.

2) Background suppression: The cell segmentation procedure uses color information. Colored background influences the appearance of color in non-background regions. In order to suppress the effect of background color we assume a multiplicative mixing of foreground and background colors. Removal of the average background color is performed separately for each color channel

$$\hat{C} = \frac{C}{\bar{C}_{bg}}, \text{ where } C \in \{R, G, B\}$$

where $\bar{C}_{bg}$ is the average background region intensity value.

3) Probabilistic leukocyte segmentation: In order to segment the leukocyte we construct a probability image which has high values for leukocyte pixels and low values for other regions. This image is segmented using an adaptive thresholding approach.

The properties of the pre-segmented regions are used to build a set of probability measures for every pixel:

- Nucleus and cytoplasm of leukocytes are stained using the same stain. It can, therefore, be expected that the hue values of both regions are similar. Experiments have shown that the initial clustering of the image provides a reliable segmentation of the nucleus regions. The measure used to determine the leukocyte hue likelihood measure for every pixel is the hue distance $dH_{nuc} = ||H - \bar{H}_{nuc}||$ where $\bar{H}_{nuc}$ is the average hue of the nucleus region.
- The clustering of the image pixels also provides a cluster which corresponds roughly to erythrocytes. The erythrocyte likelihood measure is based on $dH_{ery} = ||H - \bar{H}_{ery}||$ where $\bar{H}_{ery}$ is the average hue of the "other cells" cluster.
- The absolute values of saturation S and luminance L.

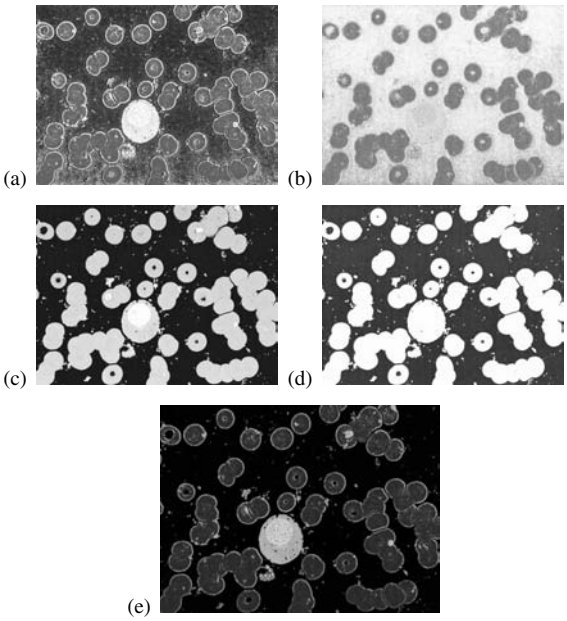

Fig. 2. Pixel likelihood measures for the image shown in Fig. 1. (a) P_{nuc}, (b) $1 - P_{ery}$, (c) P_S, (d) P_L, and (e) P_{leu}.

Each of the measures listed above is mapped into a likelihood measure P_{nuc}, P_{ery}, P_S, and P_L using a non-linear mapping function. The mapping functions have been defined using the distributions of dH_{nuc}, dH_{ery}, S, and L of a set of manually segmented leukocyte images.

In order to determine the likelihood that a single pixel belongs to a leukocyte the likelihood measures are multiplied:

$$P_{leu} = P_{nuc}(1 - P_{ery})P_S P_L$$

Sample images of pixel likelihood measures can be seen in Fig. 2.

In order to perform leukocytes segmentation it is necessary to threshold the likelihood values P_{leu}. It can be expected that a fixed threshold results in poor segmentation results for some images. Our approach to overcome fixed threshold selection is the use of maximally stable extremal regions (MSER, [5]). MSERs are obtained by thresholding an image at many (or all possible) levels. Regions obtained by thresholding are examined at multiple threshold levels. If the size change of a examined region has a local minimum (i. e. the size is nearly stable over multiple threshold levels) the region is called a maximally stable extremal region. The MSER algorithm can be applied to the leukocyte likelihood image to provide stable regions which correspond to cells or cell clusters. Combining the MSER regions with the nucleus k-means cluster allows selection of leukocytes.

4) Cytoplasm/nucleus segmentation: For classification of the leukocyte it is necessary to segment the cell into cytoplasm and nucleus. The nucleus regions provided by the initial k-means clustering procedure described above are obtained by taking into account the entire image. In some cases the nucleus regions are not sufficiently accurate

for optimum classification. Therefore, a k-means clustering ($k = 2$) is performed using HSL values of the segmented leukocyte. Morphological opening and filling of small holes is performed for the detected nucleus region.

B. Leukocyte classification

1) Color statistics features: According to medical experts texture of nucleus and cytoplasm is an important feature for discrimination of certain leukocyte types. Computation of meaningful standard texture features (e. g., Gabor features) is difficult due to the relatively small size of the leukocyte. Instead, we use the statistics of the leukocyte HSL image. The 18-dimensional feature vector is composed of mean, standard deviation, and skewness calculated separately for hue, saturation, and luminance of nucleus and cytoplasm.

2) Nucleus shape features: The shape of the nucleus region R is described by a set of simple shape descriptors [8]:

- $Convexity(R) = \frac{Perimeter(ConvexHull(R))}{Perimeter(R)}$
- Principal axis ratio: $PrAxRatio(R) = \frac{c_{yy}+c_{xx}-\sqrt{(c_{xx}+cyy)^2-4(c_{xx}c_{yy}-c_{xy}^2)}}{c_{yy}+c_{xx}+\sqrt{(c_{xx}+cyy)^2-4(c_{xx}c_{yy}-c_{xy}^2)}}$ where $\mathbf{C} = \left(\begin{smallmatrix} c_{xx} & c_{xy} \\ c_{yx} & c_{yy} \end{smallmatrix}\right)$ is the co-variance matrix of the region contour.
- $Compactness(R) = \frac{2\sqrt{\pi Area(R)}}{Perimeter(R)}$
- Circular variance: $CircVar(R) = \frac{1}{N\mu_r^2}\sum_i \left(||\mathbf{p}_i - \boldsymbol{\mu}|| - \mu_r\right)^2$, where μ_r is the mean radius, $\boldsymbol{\mu}$ is the region centroid, $\mathbf{p}_i$ is the ith contour point and N is the number of contour points.
- Elliptic variance: $EllVar(R) = \frac{1}{N\mu_{rc}}\sum_i \left(\sqrt{(\mathbf{p}_i - \boldsymbol{\mu})^T\mathbf{C}^{-1}(\mathbf{p}_i - \boldsymbol{\mu})} - \mu_{rc}\right)^2$, where $\mu_{rc} = \frac{1}{N}\sum_i \sqrt{(\mathbf{p}_i - \boldsymbol{\mu})^T\mathbf{C}^{-1}(\mathbf{p}_i - \boldsymbol{\mu})}$.

If there are multiple nucleus regions the respective shape features are averaged. In addition to these five shape features the size of the nucleus, the size of the cytoplasm and the number of detected nucleus regions are used as features.

3) SVM classification: Classification of the 26-dimensional (18 color and 8 shape) feature vector is performed with a polynomial support vector classifier [11]. An individual classifier is trained for every possible pairwise combination of the 13 classes which results in 78 classifiers.

Hard classification of a feature vector $\mathbf{x}$ is performed by $Class(\mathbf{x}) = sgn(f(\mathbf{x}))$, where $f(\mathbf{x})$ is the hyperplane function of the SVM. Hard classification is well suited for two class problems, however, for multi-class problems it is advantageous to determine a class probability measure [9]

$$P(Class|\mathbf{x}) = \frac{1}{1 + exp(-\lambda f(\mathbf{x}))}$$

where λ determines the sensitivity of the probability measure. For determining the probability of class k $P(Class_k|\mathbf{x})$ the probability measure of all classifiers involving this class are multiplied. In order to determine the class of the feature vector $\mathbf{x}$ the majority vote is used:

$$Class(\mathbf{x}) = \arg_k \max P(Class_k|\mathbf{x})$$

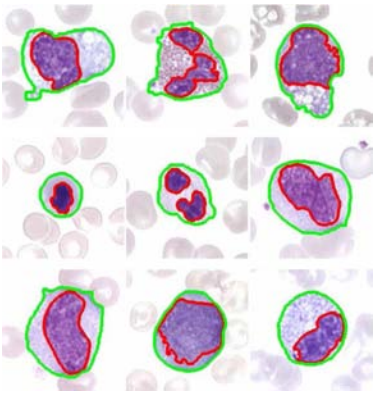

Fig. 3. Sample leukocyte segmentation results. The green line shows the leukocyte boundary, the red line the nucleus boundary.

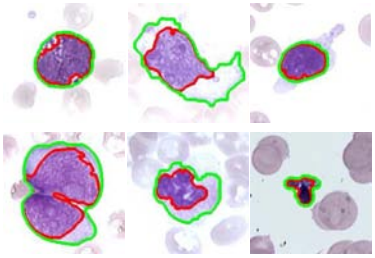

Fig. 4. Sample incorrect leukocyte segmentation results.

Samples of low probability can be assigned to the class *unknown* if $P(Class|\mathbf{x}) < T_{prob}$ where T_{prob} is a probability threshold value [2].

III. Results

The method has been evaluated using a set of 1166 images. Each image has been taken with a 63x magnification microscope and has a size of 558x750 pixels. All leukocytes have been classified by an expert.

A. Segmentation

Fig. 3 shows sample segmentation results. Out of the 1166 images 65 images contain at least one segmentation error. Segmentation errors are either incorrect leukocyte or incorrect nucleus detection (see Fig. 4 for sample images).

B. Classification

All well-segmented leukocytes were used for training and testing of the classifier. The number of cells per class can be found in Table I.

The training procedure was performed with different randomly selected disjoint training and testing sets (100 iterations). Up to 80 cells per class were used for training and at least 4 cells for testing. For training is was ensured that the size of both training sets was equal. Table I shows the classification results obtained with a polynomial ($p = 3$) SVM, a sensitivity parameter $\lambda = 4$, and a rejection threshold $T_{prob} = 0.5$. About 15.9% of all samples were rejected.

TABLE I

NUMBER OF CELL IMAGES PER CLASS AND CLASSIFICATION RESULTS WITH AND WITHOUT REJECT OPTION.

Cell type	Images	Recognition rate without reject	Recognition rate with reject
Basophil granulocyte	32	87.5%	93.8%
Myeloblast	93	82.9%	89.9%
Erythroblast	96	93.9%	96.7%
Lymphocyte	110	92.8%	97.9%
Metamyelocyte	102	74.2%	79.7%
Monocyte	103	88.4%	96.1%
Myelocyte	105	73.4%	78.3%
Plasma cell	20	67.5%	74.5%
Promyelocyte	109	78.0%	84.8%
Segmented neutrophil	104	78.9%	83.2%
Atypical lymphocyte	76	64.5%	73.0%
Eosinophil granulocyte	79	98.0%	99.5%
Band neutrophil	106	71.5%	75.8%

IV. DISCUSSION

The segmentation and classification results are good considering the wide range of image appearances. Main causes of incorrect segmentation are low nucleus/cytoplasm contrast, overexposed images, leukocyte clusters, similar leukocyte erythrocyte hue, and image artifacts (see Fig. 4). Leukocyte clusters can, for example be resolved by the method proposed in [6]. Poor image quality should be addressed during image acquisition.

For most classes the classification accuracy (with reject option) is above 90%. Misclassification occurs mainly between closely related classes. The low classification rates for plasma cells can be partly attributed to the small number of available training samples. It should, however, be noted that the classification accuracy values were obtained for visually selected sample images. In real word scenarios lower accuracy values can be expected.

The two most common leukocyte types are lymphocytes and segmented neutrophils. While the classification accuracy for lymphocytes is 98% it is only 83% for segmented neutrophils. For this class a visual inspection of the sample images showed that frequently cells lack the typical multilobed nucleus. For improved classification accuracy it should be considered to include only "typical" images in the training set. This may also improve the classification accuracy for band neutrophils. Alternative training procedures which take into account the continuous (rather than discrete) nature of the class membership or hierarchical classifiers could also be considered.

The feature dimension (26) is relatively large compared to the number of training samples (max. 80 per class). Furthermore, some of the features are partly redundant (e.g., circular and elliptic variance). Even though SVMs reduce overfitting problems it is still desirable to increase the number of training samples. Feature selection can also be considered for future improvements of the algorithm.

V. CONCLUSION

This paper presents a method for leukocyte segmentation and classification. The blood smear image is segmented into background, erythrocytes, and nucleus. Using this segmentation it is possible to calculate a leukocyte probability image based on hue, saturation and luminance values. Maximally stable extremal regions representing leukocytes are selected within this probability image. A 26-dimensional feature vector is calculated for each of the detected leukocytes. The feature vector is classified using a soft classification polynomial SVM. A sample is rejected if the class probability is below 50%. The achieved classification accuracy ranges on selected images is between 74.5% and 99.5% depending on the leukocyte class. The corresponding rejection rate is 15.9%. Future improvements can be expected from increased training set sizes. Furthermore the training data should be carefully selected to represent the "typical" appearance of a class. Feature selection and alternative training procedures (e. g. regression instead of classification) should be investigated.

ACKNOWLEDGMENT

This work has been carried out within the K plus Competence Center ADVANCED COMPUTER VISION. This work was funded from the K plus Program.

REFERENCES

[1] D. Comaniciu and P. Meer. Cell image segmentation for diagnostic pathology. In J. S. Suri, S. K. Setarehdan, and S. Singh, editors, *Advanced algorithmic approaches to medical image segmentation: state-of-the-art application in cardiology, neurology, mammography and pathology*, pages 541–558. Springer, 2001.

[2] G. Fumera, F. Roli, and G. Vernazza. A method for error rejection in multiple classifier systems. In *Proc. Int. Conf. on Image Analysis and Processing*, pages 454–458, 2001.

[3] K. Jiang, Q.-M. Liao, and S.-Y. Dai. A novel white blood cell segmentation scheme using scale-space filtering and watershed clustering. In *Proc. Int. Conf. on Machine Learning and Cybernetics*, volume 5, pages 2820–2825, 2003.

[4] Q. Liao and Y. Deng. An accurate segmentation method for white blood cell images. In *Proc. Int. Symposium on Biomedical Imaging*, pages 245–248, 2002.

[5] J. Matas, O. Chum, M. Urban, and T. Pajdla. Robust wide baseline stereo from maximally stable extremal regions. *Int. Journal of Computer Vision*, 22(10):761–767, 2004.

[6] B. Nilsson and A. Heyden. Model-based segmentation of leukocyte clusters. In *Proc. Int. Conf. on Pattern Recognition*, volume 1, pages 727–730, 2002.

[7] G. Ongun, U. Halici, K. Leblebicioglu, V. Atalay, M. Beksac, and S. Beksak. An automated differential blood count system. In *Proc. Int. Conf. of the IEEE Engineering in Medicine and Biology Society*, volume 3, pages 2583–2586, 2001.

[8] M. Peura and J. Iivarinen. Efficiency of simple shape descriptors. In C. Arcelli, L. P. Cordella, and G. Sanniti di Baja, editors, *Aspects of visual form*, pages 443–451. World Scientific, 1997.

[9] J. Platt. Probabilistic outputs for support vector machines and comparison to regularized likelihood methods. In A. J. Smola, P. Bartlett, B. Schölkopf, and D. Schuurmans, editors, *Advances in large margin classifiers*, pages 61–74. MIT Press, 2000.

[10] S. Sanei and T. K. Lee. Bayesian classification of eigencells. In *Proc. Int. Conf. on Image Processing*, volume 2, pages 929–932, 2002.

[11] B. Schölkopf, C. J. C. Burges, and A. J. Smola. Introduction to support vector learning. In *Advances in kernel methods*, book chapter 1, pages 1–15. MIT press, 1999.

[12] N. Sinha and A. G. Ramakrishnan. Automation of differential blood count. In *Proc. Conf. on Convergent Technologies for Asia-Pacific Region*, volume 2, pages 547–551, 2003.